A novel high-resolution in situ tool for studying carbon biogeochemical processes in aquatic systems: The Lake Aiguebelette case study

R. Grilli[1], T. DelSontro[2], J. Garnier[3], F. Jacob[4], J. Némery[1]

[1] Univ. Grenoble Alpes, IRD, CNRS, Grenoble INP*, IGE, F-38000, Grenoble, France

[2] Department of Earth and Environmental Sciences, University of Waterloo, Canada

[3] Sorbonne Université CNRS EPHE, Milieux environnementaux, transferts et interactions dans les hydrosystèmes et les sols, METIS, France

[4] Centre d'Ingénierie Hydraulique, EDF, France

*Institute of Engineering, Université Grenoble Alpes

Corresponding author: Roberto Grilli (roberto.grilli@cnrs.fr)

Key Points:

- Fast in situ dissolved methane and isotopic measurements
- High-resolution dissolve methane mapping
- Biogeochemical processes identification

Abstract

Lakes and reservoirs are a significant source of atmospheric methane (CH_4), with emissions comparable to the largest global CH_4 emitters. Understanding the processes leading to such significant emissions from aquatic systems is therefore of primary importance for producing more accurate projections of emissions in a changing climate. In this work, we present the first deployment of a novel membrane inlet laser spectrometer (MILS) for fast simultaneous detection of dissolved CH_4, C_2H_6 and $\delta^{13}CH_4$. During a 1-day field campaign, we performed 2D mapping of surface water of Lake Aiguebelette (France). In the littoral (pelagic) area, average dissolved CH_4 concentrations and $\delta^{13}CH_4$ were 391.9 ± 156.3 (169.8 ± 26.6) nmol L^{-1} and -67.3 ± 3.4 (-61.5 ± 3.6) ‰, respectively. The dissolved CH_4 concentration in the pelagic zone was fifty times larger than the concentration expected at equilibrium with the atmosphere, confirming an oversaturation of dissolved CH_4 in surface waters over shallow and deep areas. The results suggest the presence of CH_4 sources less enriched in ^{13}C in the littoral zone (presumably the littoral sediments). The CH_4 pool became more enriched in ^{13}C with distance from shore, suggesting that oxidation prevailed over epilimnetic CH_4 production, that was further confirmed by an isotopic mass balance technique with the high-resolution transect data. This new *in situ* fast response sensor allows to obtain unique high-resolution and high-spatial coverage datasets within a limited amount of survey time. This tool will be useful in the future for studying processes governing CH_4 dynamics in aquatic systems.

Plain Language Summary

High-resolution mapping of surface methane and its isotopic signature enables accurate characterization of aquatic systems and discrimination of biochemical processes at work. At Lake Aigueblette, this new in situ tool allowed us to conclude that methane present at the surface comes mainly from shallow littoral areas, where sediments, which are the sources of methane, are closer to the surface. During lateral transport of water masses from the littoral, the change in isotopic signature reveals that methane oxidation prevails over local *in situ* production. Comparison with previous studies validates the reliability of the high-resolution dataset and showed that, for smaller lakes, the methane isotopic signature changes faster than the methane concentration. This can be explained by the fact that the smaller lake has a larger littoral-to-total surface area. This new tool will be useful in the future to study the processes governing CH_4 dynamics in aquatic systems.

1 Introduction

Inland waters are a significant source of atmospheric methane (CH_4) (DelSontro et al., 2018a; Rosentreter et al., 2021; Saunois et al., 2019), which is a greenhouse gas (GHG) 34-85 times stronger than carbon dioxide (on 100 to 20-yr timescales including feedbacks; Myhre et al., 2013) and responsible for ~23% of global radiative forcing since 1750 (Etminan et al., 2016). Of the GHGs produced by inland waters (i.e., carbon dioxide, CH_4 and nitrous oxide), CH_4 is responsible for ~75% of the climatic impact of aquatic GHG emissions (DelSontro et al., 2018a) with aquatic CH_4 emissions comparable to the largest global CH_4 emitters - wetlands and agriculture (Saunois et al., 2019). Considering that aquatic systems contribute up to half of global CH_4 emissions (Rosentreter et al., 2021), and the fact that CH_4 is predominantly formed in anoxic environments such as lake sediments (Bastviken et al., 2004), the source and quantification of ubiquitous surface CH_4 observed in most aquatic systems are a question of global importance (e.g., Tranvik et al., 2009; Juutinen et al., 2009; Rasilo et al., 2015). As a

result, monitoring of aquatic dissolved CH_4 concentrations and emissions has steadily become more commonplace, although the methods used, particularly for investigating concentrations, remain rather manual and laboratory oriented. Concentration alone may not always be sufficient for identifying the source of surface CH_4 and the isotopic signature and/or the measurement of other short-chain hydrocarbons can significantly help to unravel the origins of the dissolved CH_4 and identify processes through which the observed CH_4 pool was potentially metabolized (Claypool and Kvenvolden, 1983).

The headspace technique (McAullife, 1971) is the manual approach most used to sample for dissolved CH_4, with concentrations later measured on a gas chromatograph (e.g., Garnier et al., 2013; Rasilo et al., 2015). Because of the manual nature of these measurements, only a few or even just one sample is often taken in systems, particularly during multi-lake surveys (e.g., Rasilo et al., 2015). Recently, however, equilibrator systems have been used to extract dissolved gas from water (either *in situ* or on site) which is then directed either to a laser-based optical spectrometer (Gerardo-Nieto et al., 2019; Gonzalez-valencia et al., 2014; Grilli et al., 2020; Wankel et al., 2013; Yuan et al., 2020) or to a compact mass spectrometer (Bärenbold et al., 2020; Brennwald et al., 2016; Short et al., 2006) for highly resolved measurements. Note that this is a not extensive list of studies. Other commercial devices for *in situ* measurements of dissolved gases are also available. For example, the METS sensor from Franatech has the advantage of being compact, low cost, and easy to use, but it relies on an indirect technique that suffers from not being gas selective, which may lead to artefacts due to presence of other dissolved gas species or to the variability of other parameters related to the water mass (*e.g.* dissolved oxygen content, temperature, salinity, hydrostatic pressure). The HydroC Contros sensor from -4H-JENA relies on the measurement of partial pressure of the dissolved gases by a Tunable Diode Laser Absorption Spectroscopy (TDLAS) technique but suffers from a slow response time (t_{90} > 30 min for CH_4) due to the membrane equilibration approach, making fast dynamic measurements impossible.

Compact quadrupole mass spectrometers are now available and led to the development and commercialization of Membrane Inlet Mass Spectrometer (MIMS) devices. These instruments provide a fast response time and a large spectrum of gas species that can be simultaneously analyzed (Nobel gases, N_2, O_2, CH_4, CO_2, H_2S, N_2O, etc.) (McMutrtry et al., 2005; Short et al., 2006; Tortell, 2005). However, the compactness of the device for *in situ* measurements limits the achievable mass resolution, leading to a problem of interference between fragments with similar mass, and making isotopic measurements nowadays still not conceivable.

With the advances on the development of optical spectroscopy sensors, and particular on cavity-based techniques, high precision concentration and also isotopic measurements are now possible using compact and transportable instruments (among others, commercial sensors are also available e.g. Picarro, Los Gatos Research, Thermo Scientific). When coupled with a dissolved gas extraction technique, these analyzers can provide *in situ* high-resolution isotopic gas measurements (Maher et al., 2015; Wankel et al., 2013; Webb et al., 2016).

It was long thought that the primary source of surface CH_4 was exclusively from anoxic sediments, either transported from littoral zones (Hofmann et al., 2010; Murase et al., 2003) or from pelagic sediments during non- or weakly-stratified periods (MacIntyre and Melack, 1995). In stratified systems, CH_4 produced in anoxic sediments diffuses into and accumulates in bottom waters but is trapped beneath a zone of minimal diffusion (Vachon et al., 2019) and oxidation (Bastviken et al., 2008), which is the primary sink for dissolved CH_4. This begs the question whether littoral sediments can adequately supply the surface CH_4 observed in most systems,

particularly in large and stratified lakes. Recent evidence suggests that CH_4 can also be produced in surface oxic waters (Bižić et al., 2020; Grossart et al., 2011) at rates sufficient enough to maintain surface CH_4 pools in a variety of systems and contribute significantly to atmospheric emissions (Günthel et al., 2019). Mass balance exercises in some systems have supported the notion that oxic methane production (OMP) can supply the majority of surface CH_4 during the stratified period (Donis et al., 2017). However, it is likely that both transport from littoral sediments and OMP maintain the surface CH_4 supply in at least most smaller lakes (DelSontro et al., 2018b). Measurements of $\delta^{13}C$ of CH_4 have provided further evidence that surface CH_4 is not only sourced from bottom waters (e.g., Donis et al. 2017) and that oxidation and an addition from another CH_4 pool (i.e., OMP) modulates the observed CH_4 pool in surface waters (DelSontro et al., 2018b). High resolution $\delta^{13}C$ measurements have the potential to offer significantly more information regarding CH_4 sources and processing in freshwaters than concentrations alone, but fast responding and high-resolution instruments for measuring $\delta^{13}C$ are lacking.

In this work, we present a first deployment of a novel membrane inlet laser spectrometer (MILS) instrument that is an upgraded version of the SubOcean probe (Grilli et al., 2018, 2020; Triest et al., 2017). A newly developed mid-infrared spectrometer for simultaneous detection of CH_4, C_2H_6 and $\delta^{13}CH_4$ (Lechevallier et al., 2019) was implemented on the *in sit*u instrument. Laboratory calibrations of the sensor are reported in the method section, followed by the results and discussions about the dissolved CH_4 data from the field campaign at Lake Aiguebelette (south east of France). Besides proving the interest of our new deployed methodology on the Lake Aiguebelette, our field investigations aimed at providing reference data on this natural peri-alpine lake in terms of CH_4 level and transformations based on associated $\delta^{13}C$ determinations.

2 Materials and Methods

2.1 Study area and field setup

The natural peri-alpine Lake Aiguebelette is located in the northern French Alps (45.5578°N, 5.8014°E) at an altitude of 374 masl (Fig. 1). The region has a sub-continental climate with mean annual rainfall of 1311 mm, and mean monthly air temperature fluctuates between 1.6 and 24 °C (OLA, 2022). The lake has a total volume of 166×10^6 m^3 with a surface area of 5.45 km^2 for a maximum and mean depth of 70 m and 30.7 m, respectively (Rimet et al., 2020). The upstream watershed surface is 59 km^2 and the water of the lake flows through the channel of Thiers to a hydroelectric plant. The lake outflow is regulated by the French Electricity Company (EDF), leading to regular fluctuations of lake level up to 0.5 m.

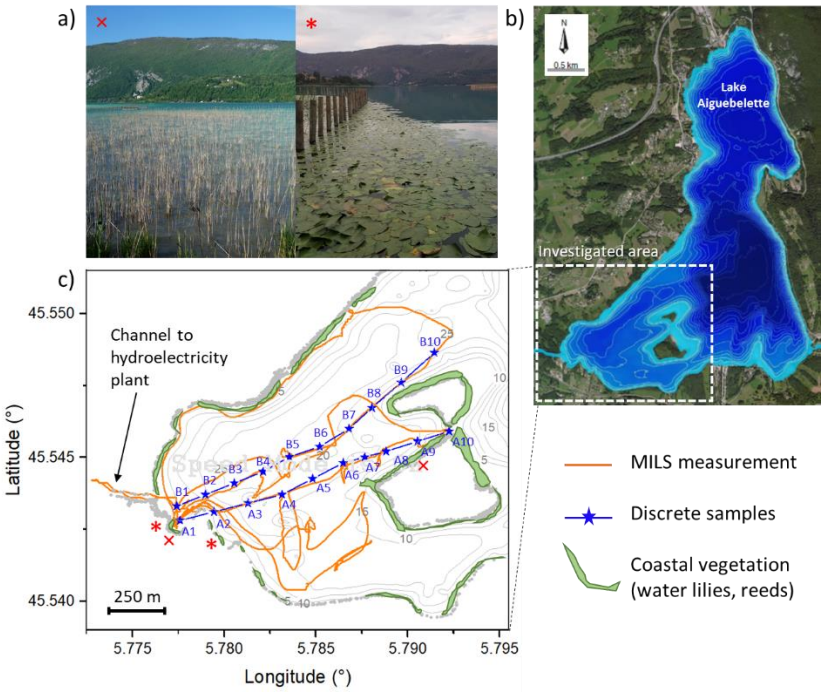

Figure 1. a) Two pictures of the vegetation: left panel: reeds, taken near the sampling point A8 – A9; right panel: water lilies taken near the sampling location A1; b) A large satellite top view of Lake Aiguebelette with the bathymetry highlighted by the 5-m isobar lines and the different depths in blue (source EDF); c) A zoom on the investigated area with the trajectories of the *in situ* MILS sensor (orange line), the location of the discrete samples along two legs (blue stars), and the coastal vegetation in green.

The lake is a warm monomictic lake that stratifies from April to November and has a mean water residence time of 3.1 years. Epilimnion depth reaches 10 m during the summer period when the hypolimnion has oxygen concentrations < 1 mgO_2 L^{-1} (Rimet et al., 2020). Like other peri-alpine lakes such as Geneva, Bourget and Annecy, Lake Aiguebelette experienced eutrophication during the 1960s and 1970s due to urbanization and touristic development. The site is now a natural area of ecological, faunistic and floristic interest listed as Natura 2000 since 2006 (NINH, 2016). A large part of the coastline (<6 m water depth) is a protected natural reserve and experiences the regeneration of a large band of macrophytes dominated mostly by reeds, with water lilies present preferentially in the southern coast of the lake. The southern coast is also more urbanized than the northern coast of the studied area (CCLA, 2017).

The measurements were carried out on May 15th 2019, at the end of a 15-day period of activity at the hydroelectric station, that lowered the water level by ~0.4 m. The continuous high-resolution MILS measurements were performed on a small electric boat equipped with GPS positioning (Garmin 18x, with an accuracy of 15m, 1σ). The boat route explored the shallow areas near the shore in the southwest of the lake to the islands in the center of the lake, then into the channel of Thiers at the lake outlet (Figure 1). A second electric boat not equipped with GPS followed the course of the first boat on legs A and B (Figure 1) in order to collect discrete water samples at 20 locations to help validate the MILS measurements. For the discrete samples, 100-ml of water was collected in a glass flask at 0-30 cm below the surface without air bubbles. To stop biological activity, 3 drops (50-80 µl) of a solution of $HgCl_2$ (i.e., 2.5-4% in final concentration) was added and the glass flask was sealed with a rubber septum excluding any headspace gas on

the field. Measurements of physical-chemical parameters were realized using a multi-parameter probe (WTW 3420®), e.g., temperature, pH, conductivity, dissolved oxygen concentration and percentage of oxygen saturation.

2.2 The MILS *in situ* sensor

The membrane inlet laser spectrometer (MILS) used here is an upgraded version of the existing SubOcean sensor that was fully described in Grilli et al. (2018). It relies on a patent-based extraction system for fast response measurements (Triest et al., 2017). The optical spectrometer, based on the optical feedback – cavity enhanced absorption spectroscopy (OFCEAS) technique (Morville et al., 2014) was working in the mid-infrared region at 3.3 μm for simultaneous detection of CH_4, C_2H_6 and $\delta^{13}CH_4$ (Lechevallier et al., 2019). The entire sensor was installed on the boat, and only the extraction unit was immerged in the water at ~50 cm depth (see Figure S1). The latter is composed by two 10 μm thick polydimethylsiloxane (PDMS) membranes of 56 mm diameter mounted face-to-face in a stainless-steel housing. The membrane block (MB) was connected to a submersible water pump (Sea-Bird Electronics, SBE 5T) that enables flushing of the membranes with a water flow of 0.8 L min^{-1}. The extraction unit was attached to the boat and connected to the probe with two 1/8", 1.2-m long flexible perfluoroalkoxy (PFA) gas pipes. A second pipe was used to inject a known flow of carrier gas (Zero Air, ALPHAGAZ 2, Air Liquide) on the dry side of the membranes. This has various purposes: i) increase the flow of gas to analyze, ii) flush the membrane in order to maintain the partial pressure difference of the target gases across the membranes at its maximum (both points increase the response time of the measurement); and iii) apply a dilution to the extracted gas to increase the dynamic range of the measurement and optimize in real time the concentration of CH_4 for the isotopic measurement. The carrier gas was stored in a 1L stainless-steal tank and a pressure reducer (Pred) and mass flow controller (MFC_{CG}, IQF+, Bronkhorst) were used for generating a controlled and constant flow of dry carrier gas. The total flow coming from the extraction system, composed of the dry dissolved gas, water vapor and carrier gas, was measured by a second mass flow controller (MFC_{TF}, IQF+ Bronkhorst) and then sent to the optical spectrometer. Prior to the MFC_{TF} a 3-port, 2-position switch valve (Burkert 6014, SV) was used for injecting from time to time a standard gas for calibrating the isotopic measurement. The setpoint of the MFC_{TF} was set 0.1 sccm (standard cubic centimeter per minute) above the maximum flow coming from the extraction unit. This allows for the use of the MFC_{TF} as a flow controller for the standard gas measurement and as a flow meter during the dissolved gas measurement.

2.3 Laboratory analysis and validation of the MILS instrument

From the 20 discrete samples collected, concentrations of CH_4 were determined by gas chromatography with flame ionization detection (Clarus 580, PerkinElmer), after creating a 30-mL headspace with N_2, as described in (Abril and Iversen, 2002; Koné et al., 2010). Certified CH_4:N_2 mixtures at 10 and 500 ppm of CH_4 were used as standards (Air Liquide, France). Repeatability was around 5%. Dissolved methane concentration was calculated with the solubility coefficient provided by Sander (2015).

The setup used to calibrate the MILS instrument in the laboratory is fully described in (Grilli et al., 2018). Similar to the field application, the extraction unit is installed in a temperature stabilized chamber and immersed in ~10 L of water. A gas mixture at known concentration of

CH_4 in air is bubbled in the water by a diffuser, and the dissolved gas concentrations were monitored continuously with the optical spectrometer. For CH_4 concentration measurements, the membrane efficiency was calculated at different water temperatures (4 – 22 °C) and salinities (0 – 31 psu) (reported in Grilli et al., 2018) and the concentrations of dissolved CH_4 were calculated from the solubility coefficients provided by Sander (2015). Calibration results for C_2H_6 are not reported here because no variation of the dissolved C_2H_6 was observed during the campaign and thus this discussion is limited to CH_4 and $\delta^{13}CH_4$ measurements. For the calibration of the isotopic measurement, three reference standards of -38.3, -54.5 and -66.5 ‰ VPDB (Isometric Instrument) were used. As observed previously (Lechevallier et al., 2019), the isotopic signature shows a dependency on CH_4 concentrations with a deviation from the true value at lower concentrations. This deviation has to be considered while retrieving the isotopic value by using the calibration curves reported in Figure 2a. Here $R^{13}C$ is the measured ratio between the $^{13}CH_4$ and $^{12}CH_4$ absorption lines, and is related to the $\delta^{13}CH_4$ through the following equation:

$$\delta^{13}CH_{4\ meas/VPDB} = \frac{R^{13}C_{meas}}{R^{13}C_{ref}} \times \left(1 + \delta^{13}CH_{4\ ref/VPDB}\right) - 1 \quad (1)$$

Where $R^{13}C_{meas}$ and $R^{13}C_{ref}$ correspond to the relative $^{13}C/^{12}C$ abundance ratios measured by the instrument for the measured and reference gas, respectively, and $\delta^{13}CH_{4\ ref/VPDB}$ is the isotopic value for the reference mixture certified against a standard material (in this case *Belemnitella americana* fossil carbonate, Vienna Pee Dee Belemnite scale). This means, for instance, that one can compute the $\delta^{13}CH_4$ for the standard at -66.5‰ by using the measured $R^{13}C$ and the certified $\delta^{13}CH_4$ of the -38.3‰ standard that will act as a reference. From the residuals between the measurement data points and the exponential fits in Figure 2a we estimated a maximum contribution by this calibration of ±0.7‰ to the final accuracy of the measurements.

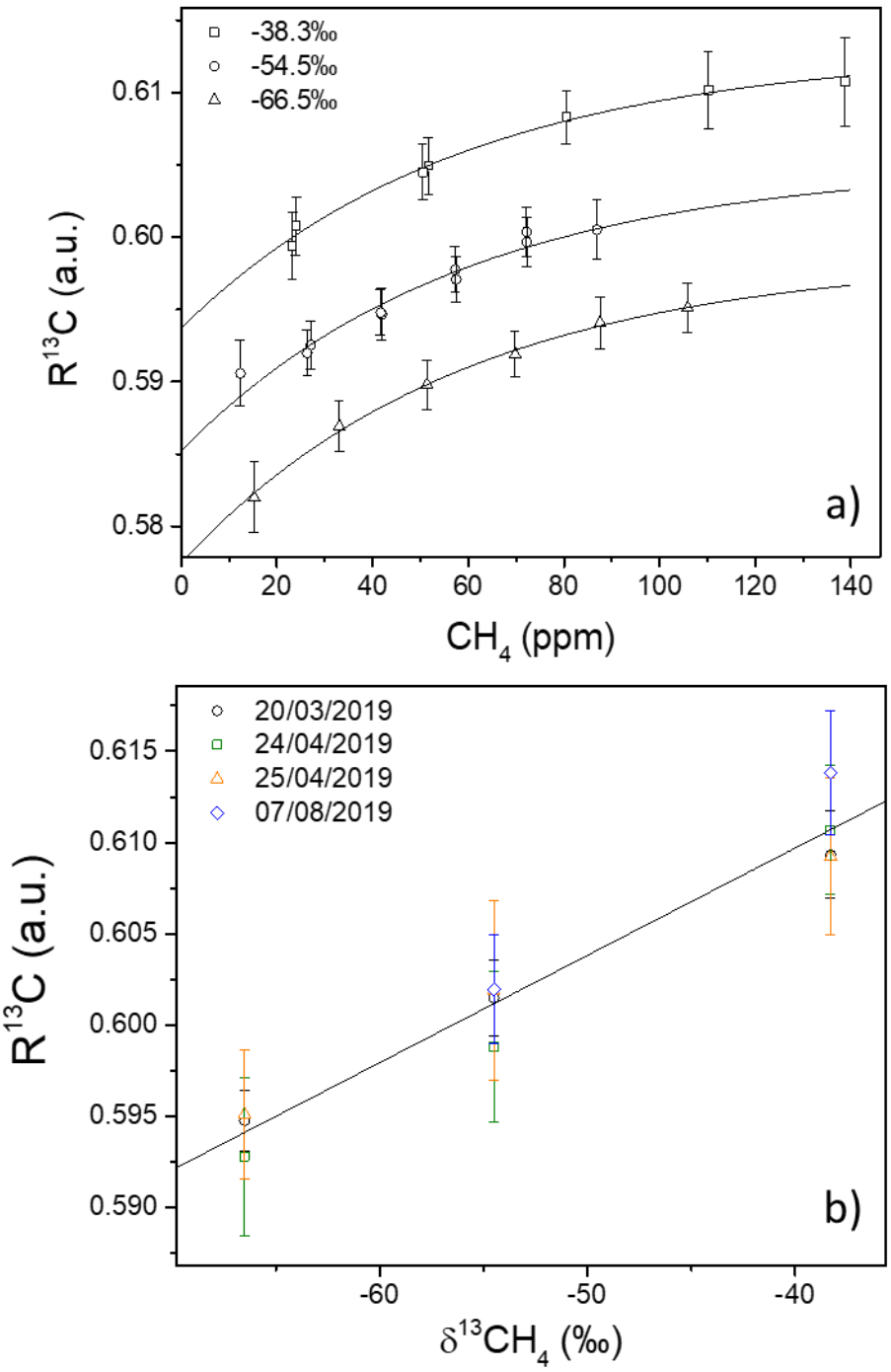

Figure 2. a) Calibration curves of the optical spectrometer for three isotopic standard mixtures showing the dependency of the abundance isotopic ratio with the concentration of CH_4. This dependency is due to an instrumental (spectral fit related) artefact that has to be considered while retrieving the $\delta^{13}CH_4$ values. b) A long-term stability test of the optical spectrometer. Measurement of the three standard mixtures was performed at different days. The spectrometer was switched off between each series of measurements. It should be noticed that the $R^{13}C$ was not referenced to a

standard mixture; therefore, the scattering of the datapoints represents the worst precision one can expect from a set of measurements referred to the same reference measurement.

In order to prove the long-term stability of the system for retrieving the isotopic signature of CH_4 we performed the measurements of the three isotopic standard mixtures at ~100 ppm of CH_4 during different days. Between each series of measurements, the instrument was switched off. The results are reported in Figure 2b. It should be noted that the plot reports the $R^{13}C$ value which is not referenced to a standard mixture. By applying equation 1 to the dataset, the corresponding variability in the $\delta^{13}CH_4$ ranged between ±2 and ±3.3 ‰ (1σ), which represents the accuracy of the optical spectrometer on the $\delta^{13}CH_4$ unreferenced to a measured standard mixture. This accuracy can be reduced to ±0.2‰ (1σ) by averaging the data for ~10 min (Figure 3 in Lechevallier et al., 2019), but also by injecting a reference gas standard for a further ~10 min in order to prevent the accuracy of the measurement to be degraded by instrumental drifts. This, however, is at the price of degraded spatial resolution of the measurements. The same figure in Lechevallier et al. (2019) shows as well that by locking the position of the cavity modes with respect to the position of the absorption lines (which was the case for the field campaign at Lake Aiguebelette), the spectrometer exhibits a much longer stability. Despite long-term drifts that start to arise after ~17 min, the precision of the measurement stays below ±1 ‰ (1σ) for 12h. We can therefore claim an accuracy of the optical spectrometer of ±0.8 ‰ (1σ) during the 9h of continuous survey.

For an accurate isotopic measurement, water conditions also have to be considered because a change in the water temperature will affect the isotopic fractionation at the membrane. This is related to the fact that after adsorption and permeation through the membrane, the gas will be desorbed, which is equivalent to an evaporative process causing a mass dependent fractionation. This effect was estimated in the laboratory, using the same calibration setup explained above. In the water where the MB was immerged, a gas mixture with a known concentration and isotopic signature of dissolved CH_4 in dry air was continuously bubbling while tuning the water temperature from 23 to 8°C and continuously monitoring the $R^{13}C$. The results are reported in Figure S2, showing an effect of the water temperature on the isotopic measurement of 0.6 ‰ per °C on the $R^{13}C$, which corresponds to 0.9 ‰ per °C on the $\delta^{13}CH_4$. The calibration was less critical for this particular campaign since the instrument only measured surface water with a stable temperature of 14.5 ± 0.2 °C during the entire campaign, which corresponds to an added uncertainty of ±0.2‰ to the final accuracy estimation of the $\delta^{13}CH_4$ measurement.

According to the dependency of the $\delta^{13}CH_4$ on the CH_4 concentration and water temperature and on the results on the repeatability of the $\delta^{13}CH_4$ measurements, we can therefore claim a final accuracy of the *in situ* $\delta^{13}CH_4$ measurements of ±1 ‰ (1σ), while for the measurement of the dissolved CH_4 concentration the precision was previously estimated to ±12 % (1σ), largely limited by the accuracy on the measurement of the carrier gas and total gas flows (Grilli et al., 2018).

2.4 Performance of the MILS sensor in the field: reproducibility and comparison with discrete measurements

During the field campaign, reference standard gas measurements with the embedded gas standard mixture (see the description of the MILS sensor in section 2.2) were conducted with the MILS instrument at different times of the day. The standard deviation of these reference

measurements was ±2 ‰, which agrees with the ±1 ‰ precision mentioned above and resulting from the calibration experiments and propagation errors. This confirmed that the optical spectrometer was sufficiently stable over the 9h of survey.

At 4:37 pm local time, we travelled ~320 m into the narrow channel on the South-West side of the basin that leads to the hydroelectric plant, and then returned along almost the same exact track over a 15-minute period (Figure S3). The similarity in concentration and isotopic results reported in Figure S3 highlights the good reproducibility of the sensor in real conditions.

At the entrance of the channel (right-hand side of the lower plots in Figure S3), the isotopic signature shows a discrepancy up to 3 ‰. This discrepancy is however not far from the accuracy of the instrument for the measurement of the $\delta^{13}CH_4$, and could also be related to a change in water mass at the entrance of the channel between the beginning and the end of the profile. It should be noted that during the measurements the hydroelectric plant was discharging water at about 1 $m^3\ s^{-1}$. Despite that minor discrepancy in the $\delta^{13}CH_4$, good reproducibility in both dissolved CH_4 and $\delta^{13}CH_4$ measurements was observed from the record in the channel.

Water sampling was conducted at different locations along two legs (Figure 1c) and analyzed in the laboratory by the headspace technique in order to compare the results with the *in situ* dissolved gas measurements performed by the MILS sensor (Figure 3). The two data sets are generally in good agreement, except for at A1 where the MILS observed a higher dissolved CH_4 concentration than the discrete water sample analysis (390.1 ± 46.8 and 213.5 ± 10.7 nmol L^{-1}, respectively). This may be explained by different reasons. First, the discrete water sampling was performed with a second boat not equipped with a GPS unit that was following the course of the first boat; therefore, the two concentrations may not have been observed at the exact same location. Figure 4a emphasizes this point as one can see the strong heterogeneity in surface water CH_4 content within 20 m distance. Thus, even small offsets in location would be critical for method comparison propose in nearshore zones due to the strong variability of surface dissolved CH_4 concentrations. Position accuracy becomes less critical further away from the shore as concentrations decrease (Figure 4b). A second possible reason for the discrepancy at A1 (Figure 3) comes from the fact that the extraction unit for the MILS sensor was at 50 cm depth, while discrete water sampling was performed between 0 and 30 cm depth. This 20-50 cm difference in sampling depth is likely to cause discrepancies between methods when sampling at shallower nearshore depths where, as already stated, large concentration gradients can be present. Finally, the discrepancy could also be related to a combination of the two hypotheses.

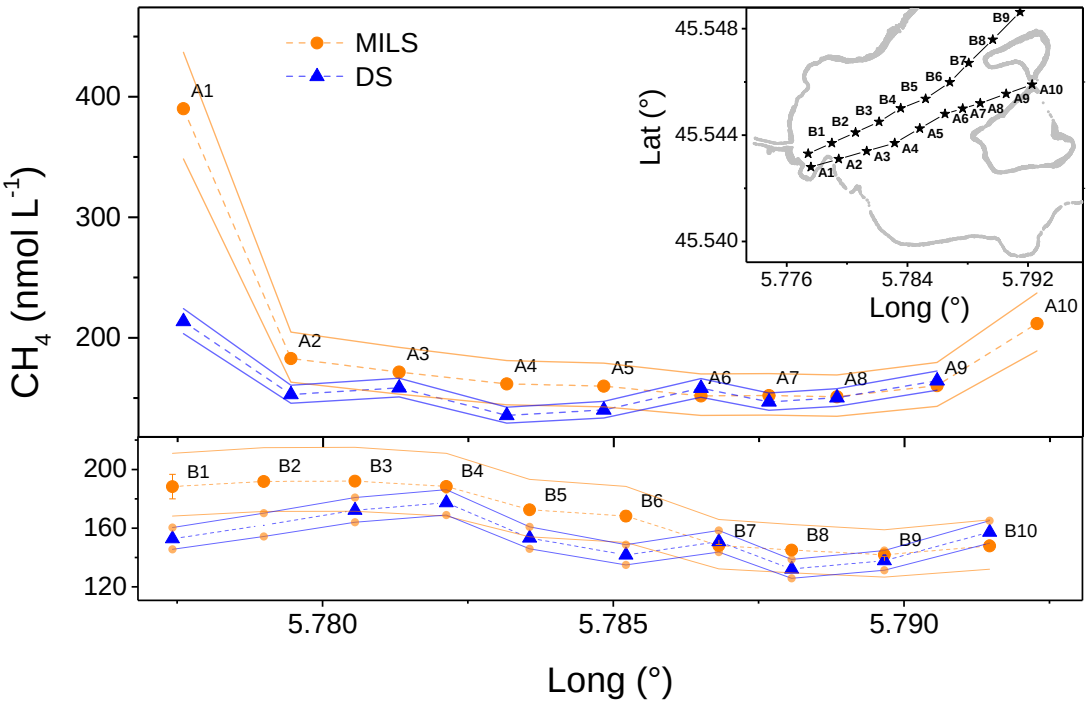

Figure 3. Comparison of dissolved methane measurements performed by the standard methods (discrete water sampling, DS, followed by laboratory headspace analysis, blue triangles) and *in situ* measurements performed by the MILS instrument (orange dots) along A and B legs. Error bars of ±5 and ±12%, respectively, are reported by solid lines and discussed in the material and method section. In the in insert the map with the sampling and measurement locations (black stars) as well as the margins of the basin (in grey).

3 Results and Discussion

3.1 Spatial distribution of CH_4 and $\delta^{13}CH_4$ in Lake Aiguebelette

The 2D maps in Figure 4 report the spatial variability of the dissolved CH_4 and its isotopic signature. The thickness of the colored line was chosen in order to have a better graphical visualization, while trying to be realistic with the possible uncertainty in the GPS position (~15m, 1σ). Dissolved C_2H_6 was also measured simultaneously, but the 2D map is not reported since the signal was very stable over the entire campaign with a mean value of 2.0 ± 0.1 nmol L^{-1}. Dissolved C_2H_6 does not correlate with either the concentration of dissolved CH_4 or the $\delta^{13}CH_4$. The shore of the lake was defined by where water depth was < 1m (black dots in Figure 4).

All observed dissolved CH_4 concentrations were above saturation in our study area. The dissolved gas concentration in the pelagic zone, where concentrations were the lowest observed, is fifty times larger than the concentration of dissolved gases expected at equilibrium with the atmosphere (3.4 nmol L^{-1} at survey temperature of 14.5 °C).

The highest concentrations of dissolved CH_4 (400 - 920 nmol L^{-1}) were observed along the shore southeast of the channel in small bay (red area on Figure 4a) and corresponded with slightly

more negative $\delta^{13}CH_4$ values (-68.6 ± 3.3 ‰) with respect to the average value in the pelagic zone (-60.7 ± 1.4 ‰). In this area at very shallow depths (< 3m) spontaneous ebullition was observed, which explains both high CH_4 concentrations and a more negative isotopic signature. Further southeast of that location and ~80 m offshore was an area with the most enriched $\delta^{13}CH_4$ values (-51.3 ± 1.3 ‰; red patch in the Figure 4c) and relatively low dissolved CH_4 concentrations (155.0 ± 3.5 nmol L^{-1}), although it was situated between two locations with elevated dissolved CH_4 concentrations (200 - 300 nmol L^{-1}). The ^{13}C-enrichement in this area as to be related to a stronger biological activity, which may be related to the urbanization of this coastal area or to the presence of a large and dense patch of macrophytes (water lilies, see picture in Figure 1a). Water lilies are also present near the sampling location A1, but in this area an isotopic composition closer to the one expected in the sediments is found most probably due to presence of gas ebullition. On the north shore of the lake, concentrations were consistently higher (192 ± 7 nmol L^{-1}), and $\delta^{13}CH_4$ more negative (-65.9 ± 1.8 ‰) than the average concentration and isotopic composition near the islands and in the middle of the lake (147.2 ± 3.4 nmol L^{-1}; 61.4 ± 1.8‰). In average, the CH_4 concentrations in the pelagic zone (> 75m from shore) were 2.7 times lower (37%) than in the littoral zones (<10m from shore) of the study area (160.8 ± 14.2 nmol L^{-1} vs 435.0 ± 174.5 nmol L^{-1}, respectively, Table 1), while the lightest $\delta^{13}CH_4$ values were in the northern part of the study area along the shore and the heaviest in the southern part just offshore.

Littoral zones of most lakes tend to be hot spots of CH_4 production, accumulation, and emission for several reasons. First is that shallow waters allow for warming of surface sediments and consequent production (Yvon-Durocher et al., 2014). While degradation rates are likely slow during cold winter temperatures, decomposition rates start to increase as spring temperatures begin to warm the shallow littoral sediments first. Thus, our May campaign led to rather high CH_4 concentrations, possibly an order of magnitude higher than what would have been observed in winter (cf. Zhang et al., 2021). Secondly, littoral zones tend to be CH_4 hot spots because the shallow sloping sediments of a littoral zone, such as that of our study area, can be a receptacle for organic carbon from algal and macrophyte biomass throughout the growing and dying seasons. This increase in organic substrate, combined with warm temperatures, leads to higher rates of methanogenesis than the pelagic. The littoral zone of Lake Aiguebelette and the islands have indeed a large band (from 5 m to 25 m wide) of rooted emergent aquatic macrophytes such as water lilies and reeds (density between 100-400 rods) (CCLA, 2017).

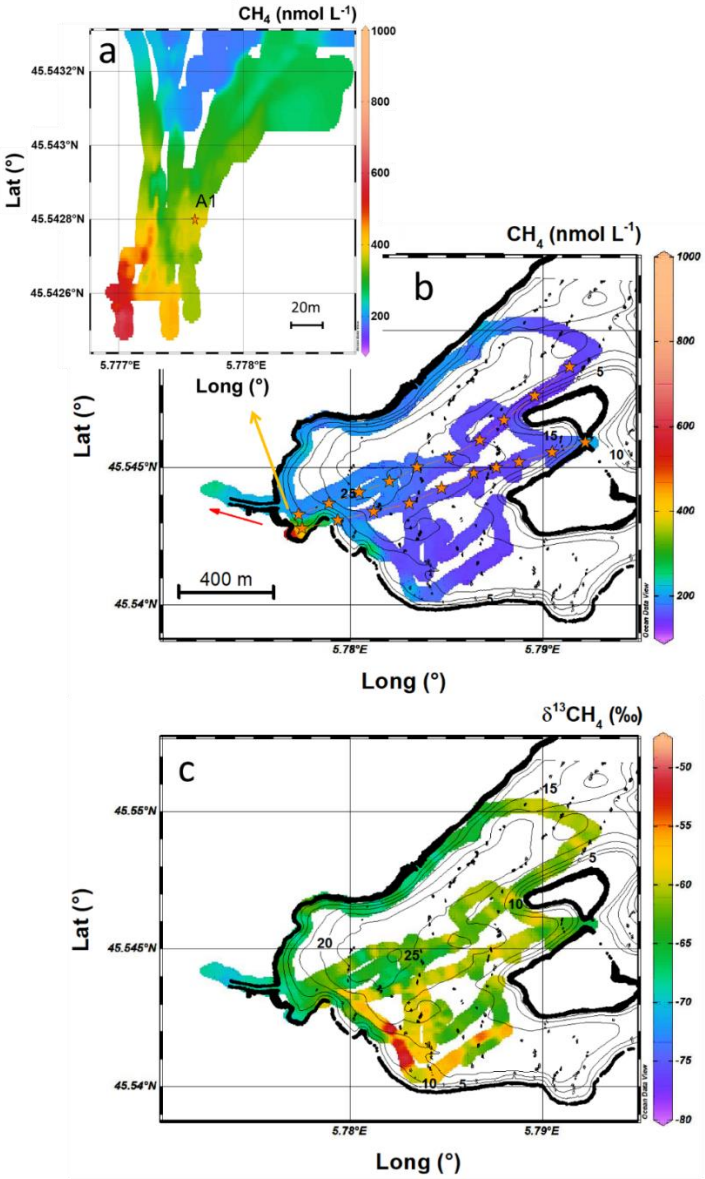

Figure 4. 2D maps of the dissolved CH_4 concentrations (a and b) and $\delta^{13}CH_4$ (c). The red arrow indicates the water flow in the exit channel of the lake and the orange starts the location of the discrete water samplings. (a) is a zoom of the area near the sampling station A1 with high dissolved CH_4 concentrations and highest concentration gradients. Black dots in (b) and (c) are the <1m depth contour line, which we defined as the shoreline.

The productivity of littoral macrophytes has major implications for CH_4 release through the accumulation of detritic organic matter in sediment (Desrosiers et al., 2022; Juutinen et al., 2003). The increase of organic content in sediment of the macrophyte regions during and following the growing period can lead to intense mineralization and depletion of oxygen in sediment (Gaillard et al., 1987; Milberg et al., 2017; Phillips et al., 2013), conditions favorable for methanogenesis. Conversely, in the deeper part of the lake that has a lower sediment surface-to-water volume ratio than the littoral, less organic carbon would reach the bottom, of which some of it would already be partially aerobically decomposed (Steinsberger et al., 2020). As the bottom water of Lake Aiguebelette is still somewhat oxic (~3 mg/L), significant aerobic

degradation would occur during particle settling and even in the slightly oxic surface sediments. Although, in general, decomposition will remain slow in the consistently cold bottom waters of this 70 m deep lake (Gudasz et al., 2010), and much of the CH_4 that is produced and then released will likely be oxidized (Bastviken et al., 2002). Ultimately, this type of functioning would support relatively low CH_4 concentrations for most of Lake Aiguebelette surface water, except for the shallow littoral zones as highlighted by our measurements.

3.2 Isotopic signature for identification of biogeochemical processing

The light isotopic signature of the CH_4 along the northern shore of the study area reflects fresh CH_4 production in the littoral zone while the slightly heavier CH_4 pool towards the islands reflects oxidized CH_4, both of which are consistent with what has been observed elsewhere (*e.g.*, DelSontro et al. 2018b). We therefore investigated the relationship between CH_4 concentration and $\delta^{13}CH_4$ with the distance from shore (DelSontro et al., 2018b). Two trends are shown in Figure 5: (i) both CH_4 and $\delta^{13}CH_4$ are relatively flat and constant at distances > 75 m from the shore with average values of 160.8± 14.2 nmol L^{-1} and -60.7 ± 3.3 ‰, respectively; (ii) CH_4 then rapidly increases near the shore, showing a larger scattering at a distance <10 m, with an average of 435.0 ± 174.5 nmol L^{-1}, highlighting that a large variability can be found nearby the shore depending on the type of sediments and vegetation as well as variability in the water depths (this is also visible in the 2D map of Figure 4a).The $\delta^{13}CH_4$ starts to decrease at distance < 75m, and it also shows a larger scattering of the data at a distance <10 m, with a mean value of -67.6 ± 3.7 ‰.

The decreasing concentration with distance from shore (Figure 5-a) indicates that CH_4 sources are closer and/or more intense in the littoral zone. The presence of a CH_4 pool nearshore that is less enriched in ^{13}C (Figure 5b) further supports the concentration trend, i.e. indicating that littoral waters are closer to CH_4 sources, which are presumably the littoral sediments. Seeing as this nearshore water can be advected offshore, the fact that the CH_4 pool becomes more enriched in ^{13}C with distance from shore suggests that the CH_4 pool have been oxidized while travelling away from the littoral.

While the trend of a decrease in concentration and an enrichment of $\delta^{13}CH_4$ from the shore towards the center of the lake is obvious, there is a high degree of variability in concentration and, to a lesser degree, in $\delta^{13}CH_4$ near shore. The variability in concentration is similar to that seen in nearshore sampling in other studies, particularly in vegetated habitats (Desrosiers et al., 2022).

The high-resolution data collected here allowed us to identify a strong non-linearity at low concentrations while relating [CH_4] and $\delta^{13}CH_4$ using Equation 12 of DelSontro et al, (2018b). Calculating the rate coefficient ($k_{O/P}$ [d^{-1}]) expressing the net impact of biological processes (oxidations and pelagic production) on surface CH_4 concentrations using only the data at high concentrations (where the linear relationship holds), we obtained a $k_{O/P}$ of 0.17 d^{-1} which is within the range of values obtained on the twelve North American lakes studied in the refered work and confirms that, at Lake Aiguebelette, oxidation prevails over pelagic production. Nevertheless, the non-linearity, which also appears to be present for four of the twelve lakes (Simard, Beauchene, Nominingue and Purvis), would require further study to understand the reasons for it and improve the modelling.

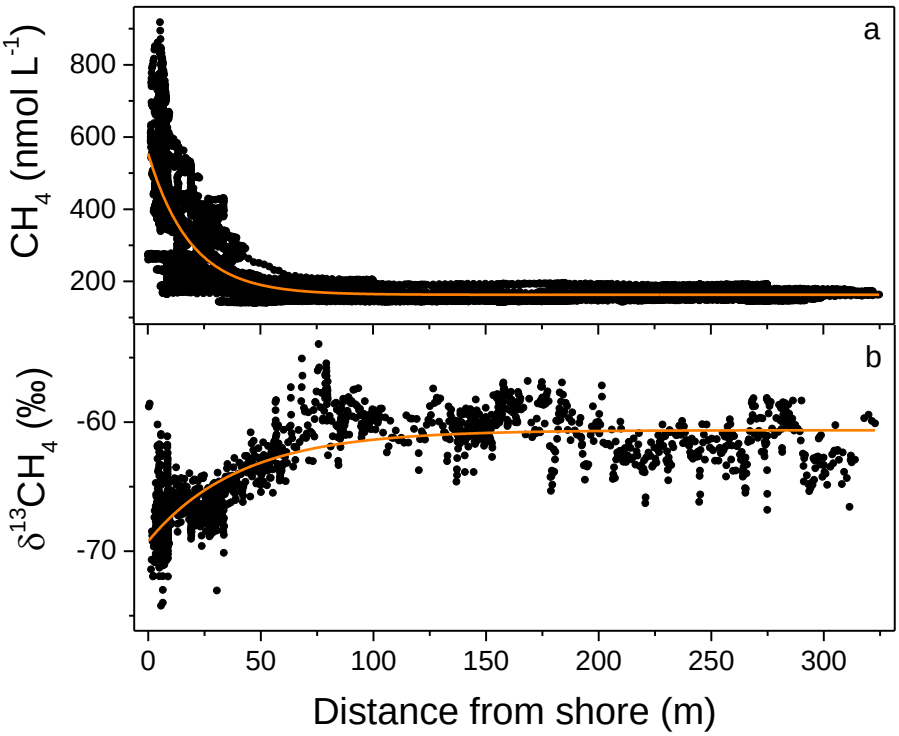

Figure 5. Distance from shore. Black dots 2 seconds data for CH_4 (a) and 20 seconds data for $\delta^{13}CH_4$ (b), orange lines are exponential fits with time constant of 18.8 m^{-1} and -40.7 m^{-1} for the CH_4 and $\delta^{13}CH_4$ trend, respectively. The data from the channel were omitted for this figure, and only the data from the lake are reported.

Table 1. Average (minimum, maximum) concentrations, isotopic composition and water depths for the entire survey area, the pelagic and the littoral zones.

		Avg CH_4 (nmol L^{-1})	Avg $\delta^{13}CH_4$ (‰)	Water Depth (m)
	Entire Survey Area	256.4 ± 147.3 (140.6 ; 922.4)	-63.7 ± 4.5 (-77.6 ; -49.6)	11.6 ± 8.4 (1 ; 26.5)
Littoral Zone	< 6m water depth	391.9 ± 156.3 (158.8 ; 922.4)	-67.3 ± 3.4 (-77.6 ; -57.0)	2.5 ± 1.6 (1 ; 6)
	<10 m from shore	435.0 ± 174.5 (165.0 ; 922.4)	-67.6 ± 3.7 (-77.6 ; -57.5)	1.3 ± 0.5 (1 ; 7.6)
Pelagic Zone	> 6m water depth	169.8 ± 26.6 (140.6 ; 339.3)	-61.5 ± 3.6 (-73.2 ; -49.6)	17.3 ± 5.4 (6 ; 26.5)
	>75m from shore	160.8 ± 14.2 (142.6 ; 208.5)	-60.7 ± 3.3 (-69.0 ; -49.6)	19.8 ± 3.7 (4.8 ; 26.5)

3.3 A broader context for Lake Aiguebelette

The work by Encinas *et al.* (2016) proposes to use the ratio of the littoral area to the area of the lake ($f_{A,S/t}$) as a metric for scaling with respect to different lakes. Here the shallow littoral was defined as the area with water depth < 6 m, and for Lake Aiguebelette this ratio is 0.1 (*i.e.*, the littoral area corresponds to 10% of the total area of the lake). From our *in situ* continuous measurements we calculated average values of CH_4 in the shallow zone ($CH_{4,s}$ = 391.8 ± 156.3 nmol L^{-1}), in the deep zone ($CH_{4,d}$ = 169.8 ± 26.6 nmol L^{-1}) and over the entire area of study ($CH_{4,t}$ = 256.4 ± 147.3 nmol L^{-1}). Those values are in good agreement with the observations reported in Encinas et al. (2016), and our data of Lake Aiguebelette nicely fit with the linear dependency in the log-log plot (predicted *vs* measured mean CH_4 concentrations) reported in Figure 3d of this referred work.

Encinas *et al.* (2016) also studied the correlation between dissolved CH_4 and Chlorophyll-a (Chl-a) concentrations. In Figure 4 of their work, they reported that the CH_4 concentration at shallow depths normalized for temperature for Lakes Illmensee and Mindlelsee are slightly below 100 nmol L^{-1} for values of Chl-a < 2 µg/L, which corresponds to annual mean values at Lake Aiguebelette (Rimet et al., 2019). In our study, we cannot estimate the dependency of the $ln(CH_4)$ with respect to water temperature (*c* parameter in the Encinas *et al.*, 2016) because we do not have data during different seasons. But if we take a representative value from Encinas et al. (2016) (c = 0.1°C^{-1}) to normalize our CH_4 concentrations then we obtain a normalized CH_4 concentration for the temperature effect (reported as $CH_{4,s}e^{-cT_s}$) of 90 nmol L^{-1}, which is in good agreement with the values of the two above mentioned lakes. Lakes Illmensee and Mindlelsee are similar to Lake Aiguebelette in terms of size and bathymetry (lake area ~1 km^2 vs 5.4 km^2; ratio of littoral to surface area, $f_{A,S/t}$ = 24-28% vs 10%), which may reinforce the hypothesis of a possible link between dissolved CH_4 and Chl-a for similar aquatic environments.

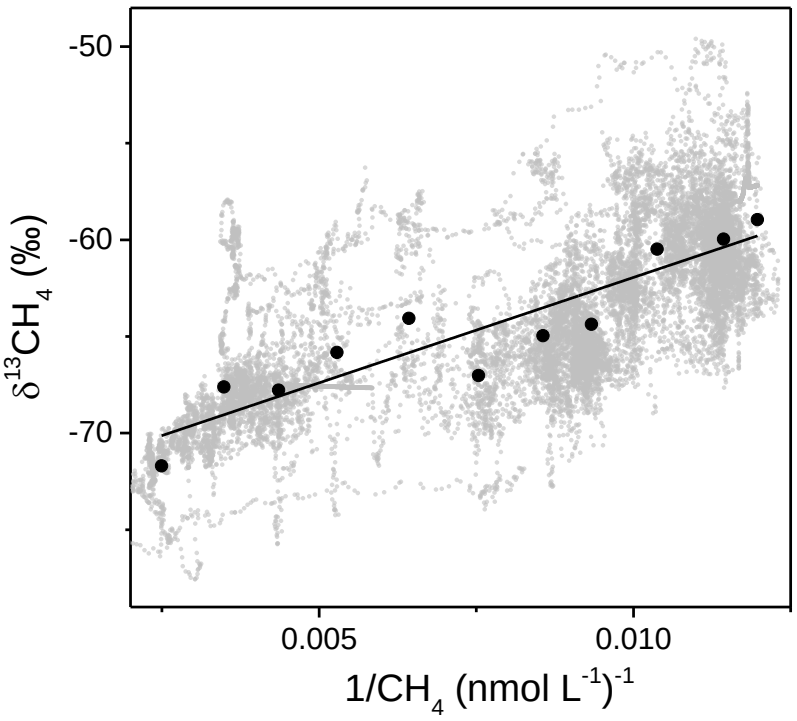

Figure 6. The isotopic composition of dissolved methane ($\delta^{13}CH_4$) plotted against the inverse of the concentration of dissolved CH_4 for continuous (grey dots) and averaged (black dots) surface water data from the campaign. The intercept at $1/CH_4 = 0$ mol^{-1} L, $\delta^{13}CH_4 = -72.8 \pm 1.22$ ‰ represents the isotopic signature at the source and the slope (1091 ± 152 ‰ nmol L^{-1}, indicate how fast the isotopic signature is changing with respect to the concentration of dissolved methane.

A method for retrieving the isotopic signature of the source of the target gas, called the Keeling plot (Keeling, 1958), consists of plotting the $\delta^{13}CH_4$ against the inverse of the dissolved CH_4 concentration and suggests that the isotopic value at the intercept ($1/CH_4 = 0$ mol^{-1} L) corresponds to the situation where the dissolved CH_4 concentrations tend to infinite values (Sasakawa et al., 2008). For our dataset, this intercept corresponds to $\delta^{13}CH_4 = -72.8 \pm 1.22$ ‰ (Figure 6), which lies at the low end of typical values observed in other lakes (*e.g.*, DelSontro et al., 2018b). The slope of that line (1091 ± 152 ‰ nmol L^{-1}) indicates how fast the isotopic signature is changing with respect to the concentration of dissolved CH_4 and provides information about the predominant CH_4 processing occurring (oxidation for positive slope, and production for negative slope), but is also related to other factors such as the possible pathway of CH_4 production, the residence time of the water mass, the presence of different CH_4 inputs, *etc*. In order to investigate the relationship between surface CH_4 and its $\delta^{13}C$ signature, we used the data from twelve Northern America lakes in DelSontro et al. (2018b) and calculate the Keeling slope for each of them. We found a negative relationship between the absolute value of the Keeling slope and lake area (Figure 7) that is likely explained by the fact that smaller lakes have a larger littoral-to-total area ratio, where methane production is likely the most active. Littoral surface waters are closest to anoxic sediments where methanogenesis occurs as well as zones of macrophytes that have a significant influence on CH_4 concentrations and may even contribute to oxic methane production (Hilt et al., 2022). Nevertheless, littoral surface waters are covered by oxic water that penetrates into surficial sediments and might promote oxidation. All of these

processes lead to changes in $\delta^{13}CH_4$, which are therefore more pronounced in smaller lakes because of that larger littoral fraction.

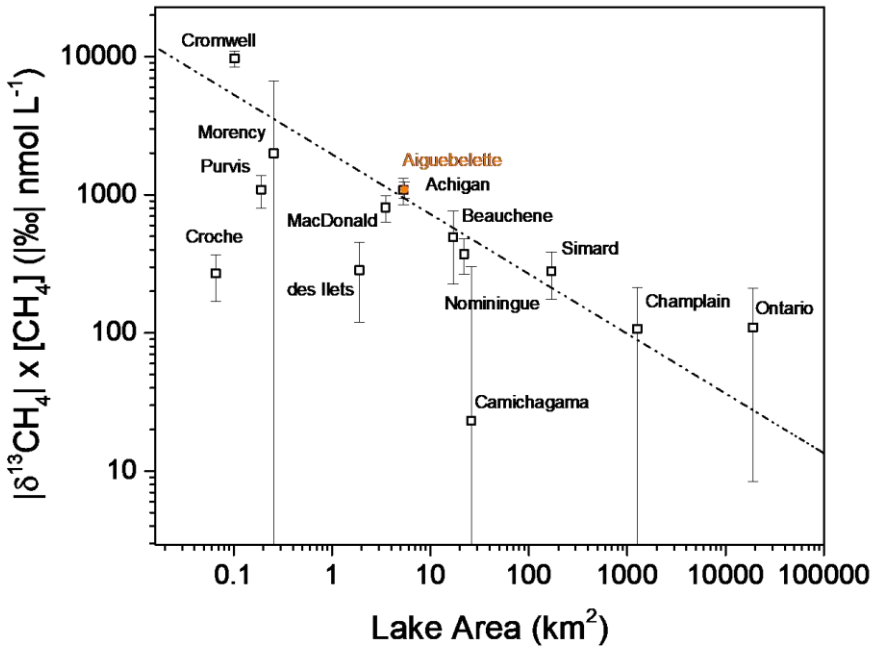

Figure 7. A log-log plot of the absolute value of the slopes calculated while plotting the $\delta^{13}CH_4$ vs the inverse of the CH_4 for the different lakes against the lake area. Data from Lake Aiguebelette (this work) is reported in orange. Data from the other lakes are from DelSontro et al., (2018b). R^2 = 0.60.

4. Conclusion and Future Works

We used an *in situ* fast response sensor for continuous, high-resolution measurements of dissolved gases to create a 2D surface map of dissolved CH_4 and $\delta^{13}CH_4$ of the southern portion of Lake Aiguebelette. The MILS sensor has an accuracy of ± 12% for dissolved CH_4 concentration measurements (against ± 5% for discrete measurements) and of ±1 ‰ (1σ) for the $\delta^{13}CH_4$. CH_4 concentration data between discrete samples and the *in situ* MILS sensor are in good agreement. The isotopic results of the MILS sensor enable to investigate the biological processing of surface CH_4 at a higher spatial resolution than discrete samples allow. At lake Aiguebelette we can conclude that CH_4 oxidation is the dominant biological process reducing the surface CH_4 pool in this lake in spring, and hence reducing some CH_4 emissions. In this work, we were able to compare our surface CH_4 and $\delta^{13}CH_4$ trends with respect to discrete data from twelve other lakes in North America. Lake Aiguebelette data followed the same trend as the majority of these data, with a decreasing CH_4 concentration with distance from shore. The comparison of these data highlights a dependency of the changing rate of isotopic ratio with respect to CH_4 concentration which decreases as a function of lake size, which is related to the fact that smaller lakes tend to have larger biologically active littoral zones relative to total lake area. This multi-lake analysis comes to reinforce the reliability of the *in situ* MILS

measurements, which allows for a reduction in measurement time while significantly improving the resolution and spatial covering of the measurements.
This new in situ methodology has several advantages over the traditional water sampling followed by laboratory analysis. First, the MILS sensor allows higher spatial resolution because it is not limited by the number of samples and time for the analysis. This spatial resolution is especially important for the littoral zone, which shows a high degree of variability both in terms of CH_4 concentration and isotopic signatures. The *in situ* instrument provides therefore a more representative estimate of a water body than discrete sampling. Secondly, the MILS sensor avoids possible artefacts due to outgassing during water sampling as well as degradation of the sample during storage (e.g., bacterial degradation or outgassing due to possible leaks). Finally, the fast deployment of the MILS system means that it is easier to conduct regular surveys and better resolve seasonal trends in aquatic CH_4. Although not illustrated in this study, the MILS sensor also allows *in situ* measurement with depth. Thus, vertical profiles at multiple locations could be conducted to better constrain CH_4 dynamics and the migration of water masses, as well as provide a more comprehensive view of how CH_4 contributes to the carbon cycle in aquatic systems.

Authors contributions

JN was the coordinator of this project in collaboration with EDF and FJ. JN organized the measurement campaign, and was the on-site mission leader. He collected the water samples for analysis in the laboratory and ensured their storage. FJ participated in the measurement campaign and provided the documents on the Lake Aiguebelette, the bathymetry data and the information on the activity of the hydro-electric power station. JG performed the analysis of the water samples in the laboratory and contributed to the interpretation of the data. RG designed, developed, calibrated and deployed the MILS instrument. He also did the data processing and coordinated the interpretation of the results and the writing of the paper. TD contributed to the data interpretation and provided the data from previous campaigns. RG, TD, JN and JG actively contributed to the writing of the paper.

Acknowledgments

This study was funded by agreement N° FUGA-UGA-2019-001 between University Grenoble Alpes Fundation and EDF and by the French National Program (ANR) “Investment for Future - Excellency Equipment” project TERRA FORMA with the reference ANR-21-ESRE-0014 ". The optical spectrometer of the MILS and the work carried out at IGE was financed thought the European Community’s Seventh Framework Programme 598 ERC-2015-PoC under grant agreement no. 713619 (ERC OCEAN-IDs), the Agence 599 Nationale de la Recherche (ANR) under grant agreement ANR-18-CE04-0003-01 (SWIS), with support from the SATT Linksium of Grenoble, France, of the Service Partenariat & Valorisation (SPV) of the CNRS.
We thank the Communité de Commune du Lac d'Aiguebellete (CCLA) for the loan of the electric boat to carry out the sampling campaign, and Arthaud's family for their nice house nearby the lake. The authors would like to thank students and staff at IGE laboratory for their contribution during field trip. We thank Anunciacion Martinez and Benjamin Mercier for the

analysis of GHGs in METIS Laboratory. We thank Frederic Guerin from GET Lab, Véronique Vaury and Sylvain Huon from iEES lab and Didier Jezequel from IPGP currently at INRAE for the fruitful discussions.

Open Research

The data from the field campaign will be deposited in an open access repository during the reviewing process.

References

Abril, G. and Iversen, N.: Methane dynamics in a shallow non-tidal estuary (Randers Fjord, Denmark), Mar. Ecol. Prog. Ser., 230, 171–181, doi:10.3354/meps230171, 2002.

Bärenbold, F., Boehrer, B., Grilli, R., Mugisha, A., von Tümpling, W., Umutoni, A. and Schmid, M.: No increasing risk of a limnic eruption at Lake Kivu: Intercomparison study reveals gas concentrations close to steady state, edited by S. A. Loiselle, PLoS One, 15(8), e0237836, doi:10.1371/journal.pone.0237836, 2020.

Bastviken, D., Ejlertsson, J. and Tranvik, L.: Measurement of Methane Oxidation in Lakes: A Comparison of Methods, Environ. Sci. Technol., 36(15), 3354–3361, doi:10.1021/es010311p, 2002.

Bastviken, D., Cole, J., Pace, M. and Tranvik, L.: Methane emissions from lakes: Dependence of lake characteristics, two regional assessments, and a global estimate, Global Biogeochem. Cycles, 18(4), 1–12, doi:10.1029/2004GB002238, 2004.

Bastviken, D., Cole, J. J., Pace, M. L. and Van de Bogert, M. C.: Fates of methane from different lake habitats: Connecting whole-lake budgets and CH4 emissions, J. Geophys. Res. Biogeosciences, 113(G2), G02024, doi:10.1029/2007JG000608, doi:10.1029/2007JG000608, 2008.

Bižić, M., Klintzsch, T., Ionescu, D., Hindiyeh, M. Y., Günthel, M., Muro-Pastor, A. M., Eckert, W., Urich, T., Keppler, F. and Grossart, H.-P.: Aquatic and terrestrial cyanobacteria produce methane, Sci. Adv., 6(3), eaax5343, doi:10.1126/sciadv.aax5343, 2020.

Brennwald, M. S., Schmidt, M., Oser, J. and Kipfer, R.: A Portable and Autonomous Mass Spectrometric System for On-Site Environmental Gas Analysis, Environ. Sci. Technol., 50(24), 13455–13463, doi:10.1021/acs.est.6b03669, 2016.

CCLA: Community of Communes of Lac d'Aiguebelette, Etude des impacts des Act. Anthr. sur les enjeux Conserv., https://ccla.fr/, 2017.

Claypool, G. E. and Kvenvolden, K. A.: Methane and other hydrocarbon gases in marine sediment., Annu. Rev. earth Planet. Sci. Vol. 11, 299–327, doi:10.1146/annurev.ea.11.050183.001503, 1983.

DelSontro, T., Beaulieu, J. J. and Downing, J. A.: Greenhouse gas emissions from lakes and impoundments: Upscaling in the face of global change, Limnol. Oceanogr. Lett., 3(3), 64–75, doi:10.1002/lol2.10073, 2018a.

DelSontro, T., del Giorgio, P. A. and Prairie, Y. T.: No Longer a Paradox: The Interaction Between Physical Transport and Biological Processes Explains the Spatial Distribution of Surface Water Methane Within and Across Lakes, Ecosystems, 21(6), 1073–1087, doi:10.1007/s10021-017-0205-1, 2018b.

Desrosiers, K., DelSontro, T. and del Giorgio, P. A.: Disproportionate Contribution of Vegetated Habitats to the CH4 and CO2 Budgets of a Boreal Lake, Ecosystems, doi:10.1007/s10021-021-00730-9, 2022.

Donis, D., Flury, S., Stöckli, A., Spangenberg, J. E., Vachon, D. and McGinnis, D. F.: Full-scale evaluation of methane production under oxic conditions in a mesotrophic lake, Nat. Commun., 8, 1661, doi:10.1038/s41467-017-01648-4, 2017.

Etminan, M., Myhre, G., Highwood, E. J. and Shine, K. P.: Radiative forcing of carbon dioxide, methane, and nitrous oxide: A significant revision of the methane radiative forcing, Geophys. Res. Lett., 43(24), 12,614-12,623, doi:10.1002/2016GL071930, 2016.

Gaillard, J. F., Sarazin, G., Pauwels, H., Philippe, L., Lavergne, D. and Blake, G.: Interstitial water and sediment chemistries of Lake Aiguebelette (Savoy, France), Chem. Geol., 63(1–2), 73–84, doi:10.1016/0009-2541(87)90075-1, 1987.

Garnier, J., Vilain, G., Silvestre, M., Billen, G., Jehanno, S., Poirier, D., Martinez, A., Decuq, C., Cellier, P. and Abril, G.: Budget of methane emissions from soils, livestock and the river network at the regional scale of the Seine basin (France), Biogeochemistry, 116(1–3), 199–214, doi:10.1007/s10533-013-9845-1, 2013.

Gerardo-Nieto, O., Vega-Peñaranda, A., Gonzalez-Valencia, R., Alfano-Ojeda, Y. and Thalasso, F.: Continuous Measurement of Diffusive and Ebullitive Fluxes of Methane in Aquatic Ecosystems by an Open Dynamic Chamber Method, Environ. Sci. Technol., 53(9), 5159–5167, doi:10.1021/acs.est.9b00425, 2019.

Gonzalez-valencia, R., Magana-rodriguez, F., Gerardo-nieto, O., Sepulveda-jauregui, A., Martinez-cruz, K., Anthony, K. W., Baer, D. and Thalasso, F.: In Situ Measurement of Dissolved Methane and Carbon Dioxide in Freshwater Ecosystems by O ff -Axis Integrated Cavity Output Spectroscopy, 2014.

Grilli, R., Triest, J., Chappellaz, J., Calzas, M., Desbois, T., Jansson, P., Guillerm, C., Ferré, B., Lechevallier, L., Ledoux, V. and Romanini, D.: Sub-Ocean: Subsea Dissolved Methane Measurements Using an Embedded Laser Spectrometer Technology, Environ. Sci. Technol., 52(18), 10543–10551, doi:10.1021/acs.est.7b06171, 2018.

Grilli, R., Darchambeau, F., Chappellaz, J., Mugisha, A., Triest, J. and Umutoni, A.: Continuous in situ measurement of dissolved methane in Lake Kivu using a membrane inlet laser spectrometer, Geosci. Instrumentation, Methods Data Syst., 9(1), 141–151, doi:10.5194/gi-9-141-2020, 2020.

Grossart, H.-P., Frindte, K., Dziallas, C., Eckert, W. and Tang, K. W.: Microbial methane production in oxygenated water column of an oligotrophic lake, Proc. Natl. Acad. Sci., 108, 19657–19661, doi:10.1073/pnas.1110716108, 2011.

Gudasz, C., Bastviken, D., Steger, K., Premke, K., Sobek, S. and Tranvik, L. J.: Temperature-controlled organic carbon mineralization in lake sediments, Nature, 466(7305), 478–481,

doi:10.1038/nature09186, 2010.

Günthel, M., Donis, D., Kirillin, G., Ionescu, D., Bizic, M., McGinnis, D. F., Grossart, H.-P. and Tang, K. W.: Contribution of oxic methane production to surface methane emission in lakes and its global importance, Nat. Commun., 10, 5497, doi:10.1038/s41467-019-13320-0, 2019.

Hilt, S., Grossart, H., McGinnis, D. F. and Keppler, F.: Potential role of submerged macrophytes for oxic methane production in aquatic ecosystems, Limnol. Oceanogr., 1–13, doi:10.1002/lno.12095, 2022.

Hofmann, H., Federwisch, L. and Peeters, F.: Wave-induced release of methane: Littoral zones as source of methane in lakes, Limnol. Oceanogr., 55(5), 1990–2000, doi:10.4319/lo.2010.55.5.1990, 2010.

Juutinen, S., Alm, J., Larmola, T., Huttunen, J. T., Morero, M., Martikainen, P. J. and Silvola, J.: Major implication of the littoral zone for methane release from boreal lakes, Global Biogeochem. Cycles, 17(4), n/a-n/a, doi:10.1029/2003GB002105, 2003.

Juutinen, S., Rantakari, M., Kortelainen, P., Huttunen, J. T., Larmola, T., Alm, J., Silvola, J. and Martikainen, P. J.: Methane dynamics in different boreal lake types, Biogeosciences, 6(2), 209–223, doi:10.5194/bg-6-209-2009, 2009.

Keeling, C. D.: The concentration and isotopic abundances of atmospheric carbon dioxide in rural areas, Geochim. Cosmochim. Acta, 13, 322–334 [online] Available from: papers2://publication/uuid/A28C5407-A4A1-4D85-9BA9-589DE73CD49C, 1958.

Koné, Y. J. M., Abril, G., Delille, B. and Borges, A. V.: Seasonal variability of methane in the rivers and lagoons of Ivory Coast (West Africa), Biogeochemistry, 100(1–3), 21–37, doi:10.1007/s10533-009-9402-0, 2010.

Lechevallier, L., Grilli, R., Kerstel, E., Romanini, D. and Chappellaz, J.: Simultaneous detection of C2H6, CH4, and δ13C-CH4 using optical feedback cavity-enhanced absorption spectroscopy in the mid-infrared region: Towards application for dissolved gas measurements, Atmos. Meas. Tech., 12(6), 3101–3109, doi:10.5194/amt-12-3101-2019, 2019.

MacIntyre, S. and Melack, J. M.: Vertical and Horizontal Transport in Lakes: Linking Littoral, Benthic, and Pelagic Habitats, J. North Am. Benthol. Soc., 14(4), 599–615, 1995.

Maher, D. T., Cowley, K., Santos, I. R., Macklin, P. and Eyre, B. D.: Methane and carbon dioxide dynamics in a subtropical estuary over a diel cycle: Insights from automated in situ radioactive and stable isotope measurements, Mar. Chem., 168, 69–79, doi:10.1016/j.marchem.2014.10.017, 2015.

McAullife, C.: GC determination of solutes by multiple phase equilibration, Chem Tech, Jan, 46–51, 1971.

McMutrtry, G. M., Wiltshire, J. C. and Bossuyt, A.: Hydrocarbon seep monitoring using in situ deep sea mass spectrometry, Ocean. 2005 - Eur., 1, 395–400, doi:10.1109/OCEANSE.2005.1511747, 2005.

Milberg, P., Törnqvist, L., Westerberg, L. M. and Bastviken, D.: Temporal variations in methane emissions from emergent aquatic macrophytes in two boreonemoral lakes, AoB Plants, 9(4), doi:10.1093/aobpla/plx029, 2017.

Morville, J., Romanini, D. and Kerstel, E.: Cavity-Enhanced Spectroscopy and Sensing, edited by G. Gagliardi and H.-P. Loock, Springer Berlin Heidelberg, Berlin, Heidelberg., 2014.

Murase, J., Sakai, Y., Sugimoto, A., Okubo, K. and Sakamoto, M.: Sources of dissolved methane in Lake Biwa, Limnology, 4(2), 91–99, doi:10.1007/s10201-003-0095-0, 2003.

Myhre, G., Shindell, D., Bréon, F.-M., Collins, W., Fuglestvedt, J., Huang, J., Koch, D., Lamarque, J.-F., Lee, D., Mendoza, B., Nakajima, T., Robock, A., Stephens, G., Takemura, T. and Zhang, H.: Anthropogenic and Natural Radiative Forcing, in Climate Change 2013: The Physical Science Basis. Contribution of Working Group I to the Fifth Assessment Report of the Intergovernmental Panel on Climate Change, edited by T. Stocker, D. Qin, G.-K. Plattner, M. Tignor, S. K. Allen, J. Boschung, A. Nauels, Y. Xia, V. Bex, and P. . Midgley, pp. 659–740, Cambridge University Press, Cambridge, UK and New York, NY, USA., 2013.

NINH: National Inventory of Natural Heritage, [online] Available from: https://inpn.mnhn.fr/site/natura2000/FR8201770, 2016.

OLA: Observatory on Lake, [online] Available from: https://www6.inrae.fr/soere-ola_eng, 2022.

Phillips, N. G., Ackley, R., Crosson, E. R., Down, A., Hutyra, L. R., Brondfield, M., Karr, J. D., Zhao, K. and Jackson, R. B.: Mapping urban pipeline leaks: Methane leaks across Boston, Environ. Pollut., 173, 1–4, doi:10.1016/j.envpol.2012.11.003, 2013.

Rasilo, T., Prairie, Y. T. and del Giorgio, P. A.: Large-scale patterns in summer diffusive CH4 fluxes across boreal lakes, and contribution to diffusive C emissions, Glob. Chang. Biol., 21, 1124–1139, doi:10.1111/gcb.12741, 2015.

Rimet, F., Khac, V. T., Quétin, P. and De, S.: Suivi de la qualité des eaux du lac d'Aiguebelette., 2019.

Rimet, F., Anneville, O., Barbet, D., Chardon, C., Crépin, L., Domaizon, I., Dorioz, J. M., Espinat, L., Frossard, V., Guillard, J., Goulon, C., Hamelet, V., Hustache, J. C., Jacquet, S., Lainé, L., Montuelle, B., Perney, P., Quetin, P., Rasconi, S., Schellenberger, A., Tran-Khac, V. and Monet, G.: The Observatory on LAkes (OLA) database: Sixty years of environmental data accessible to the public, J. Limnol., 79(2), 164–178, doi:10.4081/jlimnol.2020.1944, 2020.

Rosentreter, J. A., Borges, A. V., Deemer, B. R., Holgerson, M. A., Liu, S., Song, C., Melack, J., Raymond, P. A., Duarte, C. M., Allen, G. H., Olefeldt, D., Poulter, B., Battin, T. I. and Eyre, B. D.: Half of global methane emissions come from highly variable aquatic ecosystem sources, Nat. Geosci., 14(4), 225–230, doi:10.1038/s41561-021-00715-2, 2021.

Sander, R.: Compilation of Henry 's law constants (version 4.0) for water as solvent, Atmos. Chem. Phys., 15, 4399–4981, doi:10.5194/acp-15-4399-2015, 2015.

Sasakawa, M., Tsunogai, U., Kameyama, S., Nakagawa, F., Nojiri, Y. and Tsuda, A.: Carbon isotopic characterization for the origin of excess methane in subsurface seawater, J. Geophys. Res., 113(C3), C03012, doi:10.1029/2007JC004217, 2008.

Saunois, M., Stavert, A. R., Poulter, B., Bousquet, P., Canadell, J. G., Jackson, R. B., Raymond, P. A., Dlugokencky, E. J., Houweling, S., Patra, P. K., Ciais, P., Arora, V. K., Bastviken, D., Bergamaschi, P., Blake, D. R., Brailsford, G., Bruhwiler, L., Carlson, K. M., Carrol, M., Castaldi, S., Chandra, N., Crevoisier, C., Crill, P. M., Covey, K., Curry, C. L., Etiope, G.,

Frankenberg, C., Gedney, N., Hegglin, M. I., Höglund-Isakson, L., Hugelius, G., Ishizawa, M., Ito, A., Janssens-Maenhout, G., Jensen, K. M., Joos, F., Kleinen, T., Krummel, P. B., Langenfelds, R. L., Laruelle, G. G., Liu, L., Machida, T., Maksyutov, S., McDonald, K. C., McNorton, J., Miller, P. A., Melton, J. R., Morino, I., Müller, J., Murgia-Flores, F., Naik, V., Niwa, Y., Noce, S., O'Doherty, S., Parker, R. J., Peng, C., Peng, S., Peters, G. P., Prigent, C., Prinn, R., Ramonet, M., Regnier, P., Riley, W. J., Rosentreter, J. A., Segers, A., Simpson, I. J., Shi, H., Smith, S. J., Steele, P. L., Thornton, B. F., Tian, H., Tohjima, Y., Tubiello, F. N., Tsuruta, A., Viovy, N., Voulgarakis, A., Weber, T. S., van Weele, M., van der Werf, G. R., Weiss, R. F., Worthy, D., Wunch, D., Yin, Y., Yoshida, Y., Zhang, W., Zhang, Z., Zhao, Y., Zheng, B., Zhu, Q., Zhu, Q. and Zhuang, Q.: The Global Methane Budget 2000-2017, Earth Syst. Sci. Data, 12(3), 1561–1623, doi:10.5194/essd-2019-128, 2019.

Short, R. T., Toler, S. K., Kibelka, G. P. G., Rueda Roa, D. T., Bell, R. J. and Byrne, R. H.: Detection and quantification of chemical plumes using a portable underwater membrane introduction mass spectrometer, TrAC - Trends Anal. Chem., 25(7), 637–646, doi:10.1016/j.trac.2006.05.002, 2006.

Steinsberger, T., Schwefel, R., Wüest, A. and Müller, B.: Hypolimnetic oxygen depletion rates in deep lakes: Effects of trophic state and organic matter accumulation, Limnol. Oceanogr., 65(12), 3128–3138, doi:10.1002/lno.11578, 2020.

Tortell, P. D.: Dissolved gas measurements in oceanic waters made by membrane inlet mass spectrometry, Limnol. Oceanogr. Methods, 3(1), 24–37, doi:10.4319/lom.2005.3.24, 2005.

Tranvik, L. J., Downing, J. A., Cotner, J. B., Loiselle, S. A., Striegl, R. G., Ballatore, T. J., Dillon, P., Finlay, K., Fortino, K., Knoll, L. B., Kortelainen, P. L., Kutser, T., Larsen, S., Laurion, I., Leech, D. M., Mccallister, S. L., Mcknight, D. M., Melack, J. M., Overholt, E., Porter, J. A., Prairie, Y., Renwick, W. H., Roland, F., Sherman, B. S., Schindler, D. W., Sobek, S., Tremblay, A., Vanni, M. J., Verschoor, A. M., Wachenfeldt, E. Von and Weyhenmeyer, G. A.: Lakes and reservoirs as regulators of carbon cycling and climate, Limnol. Oceanogr., 54(6), 2298–2314, doi:10.4319/lo.2009.54.6_part_2.2298, 2009.

Triest, J., Chappellaz, J. and Grilli, R.: Patent WO2018127516A1: System for fast and in-situ sampling of dissolved gases in the ocean (CNRS, Grenoble FRANCE), 2017.

Vachon, D., Langenegger, T., Donis, D. and McGinnis, D. F.: Influence of water column stratification and mixing patterns on the fate of methane produced in deep sediments of a small eutrophic lake, Limnol. Oceanogr., 64(5), 2114–2128, doi:10.1002/lno.11172, 2019.

Wankel, S. D., Huang, Y., Gupta, M., Provencal, R., Leen, J. B., Fahrland, A., Vidoudez, C. and Girguis, P. R.: Characterizing the Distribution of Methane Sources and Cycling in the Deep Sea via in Situ Stable Isotope Analysis, Environ. Sci. Technol., 47(3), 1478–1486, doi:10.1021/es303661w, 2013.

Webb, J. R., Maher, D. T. and Santos, I. R.: Automated, in situ measurements of dissolved CO2, CH4, and δ13C values using cavity enhanced laser absorption spectrometry: Comparing response times of air-water equilibrators, Limnol. Oceanogr. Methods, 14(5), 323–337, doi:10.1002/lom3.10092, 2016.

Yuan, F., Hu, M., He, Y., Chen, B., Yao, L., Xu, Z. and Kan, R.: Development of an in situ analysis system for methane dissolved in seawater based on cavity ringdown spectroscopy

Development of an in situ analysis system for methane dissolved in seawater based on cavity ringdown spectroscopy, Rev. Sci. Instrum., 91(083106), doi:10.1063/5.0004742, 2020.

AGU PUBLICATIONS

JGR: Biogeosciences

Supporting Information for

A novel high-resolution in situ tool for studying carbon biogeochemical processes in aquatic systems: The Lake Aiguebelette case study

Roberto Grilli[1], Tonya DelSontro[2], Josette Garnier[3], Frederick Jacob[4], Julien Némery[1]

[1] Univ. Grenoble Alpes, IRD, CNRS, Grenoble INP*, IGE, F-38000, Grenoble, France
[2] Department of Earth and Environmental Sciences, University of Waterloo, Canada
[3] Sorbonne Université CNRS EPHE, Milieux environnementaux, transferts et interactions dans les hydrosystèmes et les sols, METIS, France
[4] Centre d'Ingénierie Hydraulique, EDF, France

*Institute of Engineering, Université Grenoble Alpes

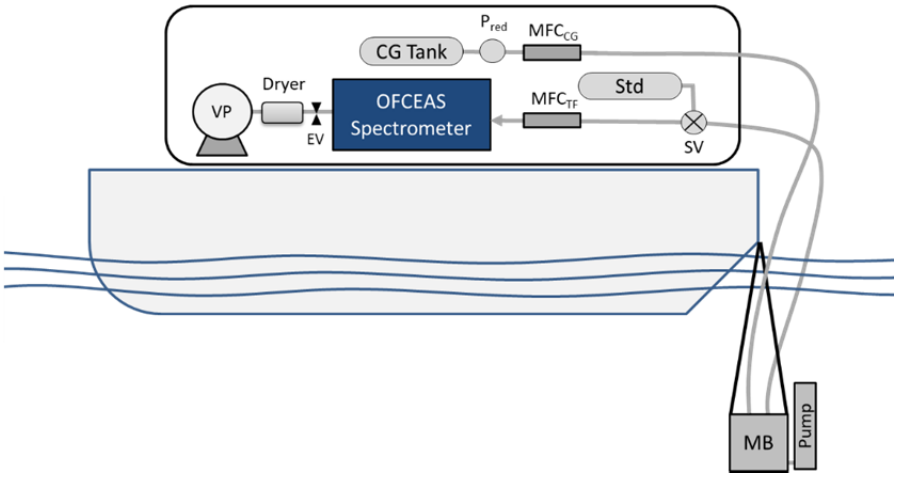

Figure S1. Schematic of the MILS (membrane inlet laser spectrometer) probe in the field. The instrument was installed on the boat while the extraction unit (composed by the membrane extraction block, MB, and a water pump) was immerged in the water at 50 cm depth. The instrument and the extraction unit were connected with 1.2 m long 1/8" PFA tubing. SV is a 3-ports 2-positions switch valve allowing to regularly inject a standard gas (std tank) at a known isotopic composition to the spectrometer for calibration propose. MFC_{CG} and MFC_{TF} were two mass flow controllers for setting the carrier gas and total gas flows. P_{red} is a pressure reducer. A vacuum pump (VP) and a solenoid proportional electrovalve EV were used for regulating the pressure in the measurement cavity, and a silica gel dryer employed for removing the water vapor before the VP.

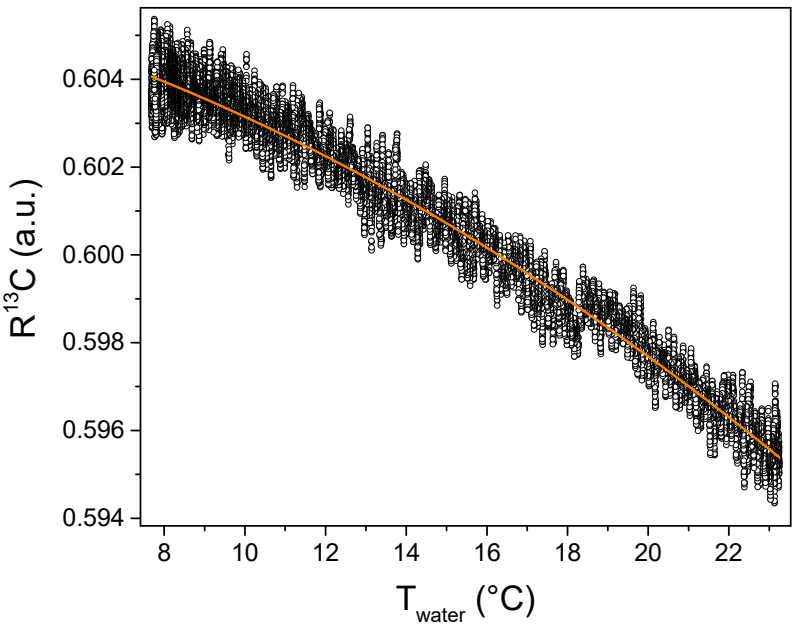

Figure S2. Dependency of the isotopic fractionation to the water temperature estimated to 0.6 ‰ per °C on the $R^{13}C$, corresponding to 0.9 ‰ per °C on the $\delta^{13}CH_4$.

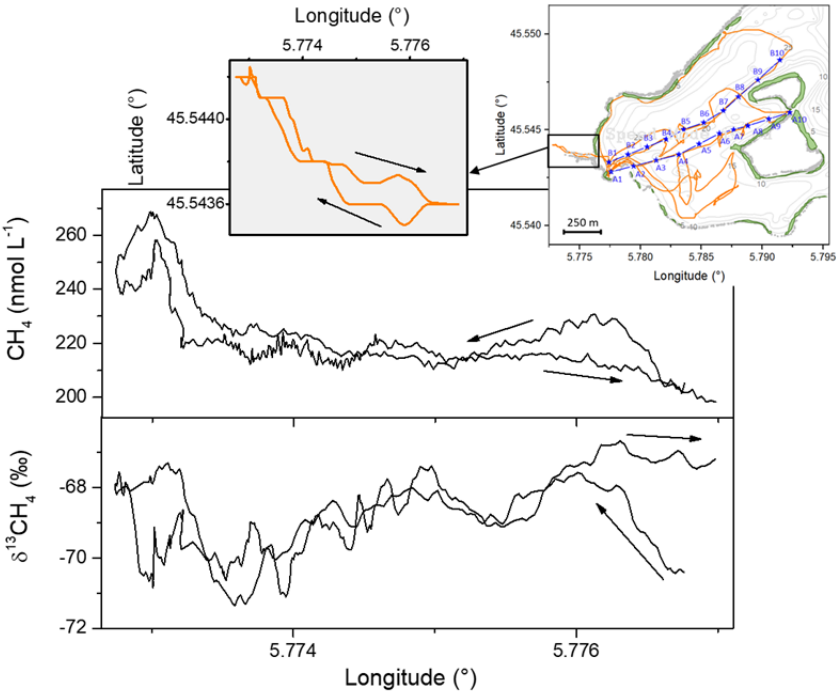

Figure S3. Reproducibility of the instrument while going back and forward in the channel (15 min continuous acquisition). Arrows indicate the direction of the time series. The location of the channel is reported in two above inserts.